

## A NEW APPROACH TO OSTWALD RIPENING : BEHAVIOUR AT EARLY STAGES AND INFLUENCE OF THE GRAIN CONNECTIVITY

GRUY F. and COURNIL M.  
Centre S.P.I.N.

Ecole des Mines de Saint-Etienne, 158 Cours Fauriel, 42023 Saint-Etienne, France

### ABSTRACT

Thanks to the unidimensional model of Ostwald ripening proposed here, the most general systems, in particular with high solid volume fraction can be studied and new aspects can be considered : influence of the spatial arrangement of the grains, first stage of ripening, influence of a non-constant mass diffusion coefficient.

Ostwald ripening, or coarsening of second phase particles is one of the major causes of changes in the particle size distribution (PSD) with time for a given population of grains. It is particularly important for processes such as ageing of precipitates or liquid phase sintering. The first models (1) and (2, 3) (LSW model) were based on several restrictive assumptions, in particular very small volume fraction of grains  $\phi$  and very dilute matrix or liquid phase. They predicted an asymptotic behaviour characterized by a cubic relationship of the mean particle size  $\bar{R}$  versus time, when mass diffusion is the rate-determining step :

$$\bar{R}^3 - \bar{R}_0^3 = Kt$$

$\bar{R}_0$  is the initial mean particle radius, K is a rate constant. A quasi stable, left-skewed, PSD was found in these studies. Many authors (4-8) tried to improve the LSW model by including the effect of the volume fraction ; they also obtained asymptotic cubic laws, however with  $\phi$  dependent rate constants. However, their models were valid only for small  $\phi$  values and could not explain the experimental shape (right-skewed) of the PSD. Other authors (9-16) took into account in a more realistic way the interaction between a given grain and its neighbours. More concentrated systems could be so studied and new PSD shapes -closer to the experimental observations- were found. Few researchers have investigated the transient preasymptotic evolution (14-16).

In this paper, we present several applications of a new mathematical and numerical tool which can be used to simulate any situation of Ostwald ripening. Compared to the so far existing models, our approach allows us to study new cases or new aspects, for instance : highly charged systems with high solubility, initial, transient and asymptotic evolution with time, influence of the spatial distribution and connectivity of the grains. This model is one-dimensionnal i.e. it considers Ostwald ripening in a row of grains. Its validity and its interest were proved in a recent paper (17), in which a detailed description can be found. The aim of the present paper is to remind the main features of the model and the associated numerical procedure and to present several possible applications ; some of them are quite new because untractable or ignored by the previous approaches. In particular, the possibility of a non constant mass diffusion coefficient is envisaged too ; for this, the theoretical and experimental results found by Myerson and co-workers (18) in supersaturated systems are applied.

### DESCRIPTION OF THE MODEL

Figure 1 represents the geometry of the unidimensional set of particles. The particles are composed of the solid A (solute), which is soluble in the liquid B (solvent). A grain  $i$  is defined by two boundaries,  $LB_i$  and  $RB_i$ . The left boundary of the whole system is fixed whereas the right boundary may be free to

move. The model can now be built according to the successive steps:

i) mass balance equations:

To be representative of dilute as well as concentrated liquid media, the mass balance equations of A must be written in the general form (19, 20) :

$$\frac{\partial \rho_A}{\partial t} = - \frac{\partial}{\partial x} \left( \rho_A v_x - \frac{D}{\rho \bar{V}_B} \frac{\partial \rho_A}{\partial x} \right) \quad (1)$$

$\rho_k$ , and  $\bar{V}_k$  are the mass density and mass partial volume respectively of component k ; D is the experimentally measured diffusion coefficient of A into B ;  $v_x$  is the mean mass velocity along the coordinate x. The total mass balance is expressed by :

$$\frac{\partial \rho}{\partial t} = - \frac{\partial (\rho v_x)}{\partial x} \quad (2)$$

where  $\rho = \rho_A + \rho_B$  is the total mass density of the liquid.

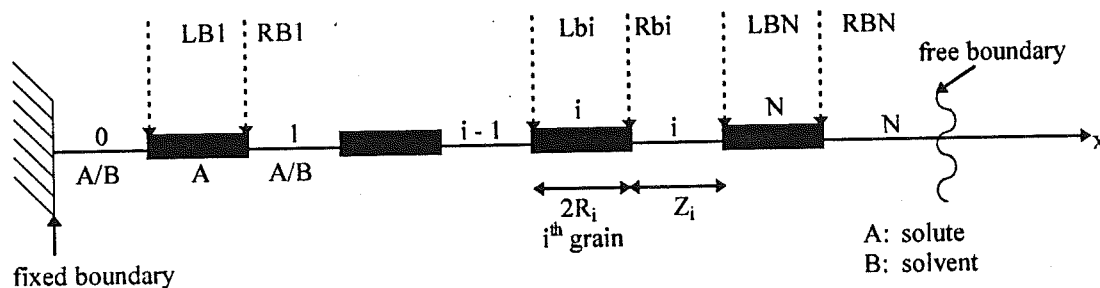


Figure 1 : Geometry of the set of particles

ii) state equation of the liquid phase:

$\rho$  and  $\rho_A$  are not independent variables, but are linked by the state equation of the liquid phase which is assumed by Pascal (21) to be expressed as:

$$\rho = \rho_B^0 + a \rho_A \quad (3)$$

$\rho_B^0$  is the density of the pure solvent ; a is an experimentally measured constant. We will consider two cases: the diffusion coefficient may be constant, as in the classical theory of Ostwald ripening, or depending on the solute concentration. For the latter case, we adopt the point of view of Myerson (18): he observes a rapid decline in diffusivity with increasing concentration in the supersaturated region. The concentration which corresponds to a zero diffusivity is the spinodal concentration  $\rho_{A,sp}$ . We will use a linear decreasing function for diffusivity versus concentration:

$$D = D_{eq}^{\infty} \frac{\rho_{A,sp} - \rho_A}{\rho_{A,sp} - \rho_{A,eq}^{\infty}} \quad (4)$$

$\rho_{A,eq}^{\infty}$  is the solute equilibrium concentration for a plane interface (grain-liquid) ;  $D_{eq}^{\infty}$  is the corresponding diffusivity.

iii) boundary conditions:

The boundary conditions may be found following Vrentas (22, 17) :

$$\rho_A (v_A - U) = \rho_S (v_S - U) \quad ; \quad \rho_B (v_B - U) = 0 \quad (5)$$

where U and  $v_S$  are respectively the velocity of the phase interface and the mass average velocity in the

solid phase.

Assuming that the surface kinetics is described by a first order law, it follows :

$$\pm \rho_S (U - v_S) = \rho_S k (\rho_A - \rho_{A,eq}) \quad (6)$$

where  $k$  is a kinetic constant,  $\rho_S$  the solid phase density, and  $\rho_{A,eq}$  the equilibrium concentration or the solubility of A given by Gibbs Kelvin law:  $\rho_{A,eq} = \rho_{A,eq}^\infty e^{\frac{\alpha}{R}}$ . The "+" sign corresponds to the interface RBi, and the "-" sign corresponds to the interface LBi.

From equations (1, 5, 6), boundary conditions at any grain-liquid interface can be obtained (17).

iv) initial conditions:  $\rho_A = \rho_{A,in}$

At instant zero, the concentration in A is assumed to be uniform in the liquid phase.

v) time evolution of the grain radii :

From the different boundary conditions (17), it follows :

$$\frac{d(2R_i)}{dt} = (U - v_S)_{x=RB_i} + (U - v_S)_{x=LB_i} \quad (7)$$

The above set of equations poses a typical moving boundary problem. Generally speaking, exact solutions of moving boundary problems are available only in a few cases. However, a number of special techniques have been developed to give an approximate solution to the problem. In the present study, we apply the simplest method i.e. : Goodman's integral approximation (23, 24, 17).

## RESULTS

In this section, we report results of numerical integration of the ODE system setup above.

The application field of our model is too large to examine all the possible cases. A set of typical parameter values commonly met in other theoretical works has been chosen :

$$\frac{\rho_{A,eq}^\infty}{\rho_{0B}} = 0.3 ; \frac{\rho_{0B}}{\rho_S} = 0.2 ; \frac{\rho_{A,in}^\infty}{\rho_{0B}} = 0.33 ; a = 0.2 ; \frac{\alpha}{L_0} = 10^{-5}$$

$L_0$  is the overall initial system size. The ratio  $L_0 \rho_S k / D$  has been so defined that it can be varied if so desired, because this parameter compares the diffusion to the interfacial reaction rate.

### GENERAL BEHAVIOUR

Constant diffusivity :  $D = D_{eq}^\infty$

For the first simulations, the initial condition is a set of randomly chosen radii uniformly distributed between 0 and  $2\bar{R}$ . The grains are randomly placed. The initial intergranular distances, either  $Z_i(0)$  or  $R_i(0) + Z_i(0) + R_{i+1}(0)$  are taken to be constant. The results are the same for the two cases.

When the interface reaction is the rate-limiting step, a parabolic law is observed for the variation of the mean radius with time. When the solute diffusion is the rate-limiting step, a cubic law is observed (Fig. 2). This is true whatever the volume fraction. This result agrees with LSW and related theories. From now on, we will deal with evolutions where the diffusion is the rate-limiting step. We have verified that a cubic law is observed not only during the period of asymptotic behaviour, to be in agreement with these theories, but also as early as the first stage of the process. This behaviour was recently mentioned by Patterson and co-workers (14, 25). The reduced PSD has been calculated for different steps of Ostwald ripening ( $\phi = 0.25$  ; Fig. 3). It tends to a quasi-stable form which is independent of the rate-limiting step. The standard deviation tends to a certain limit ( $\sigma_{qs} = 0.35$ ). The skewness is negative but small ( $S_{qs} = -0.25$ ). This indicates that the PSD shape is nearly symmetrical.

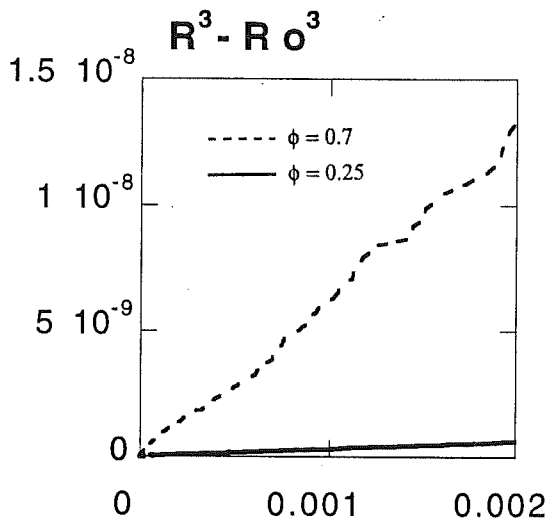


Figure 2 :  $\bar{R}^3 - \bar{R}_0^3$  versus time  $t$  (dimensionless variables)

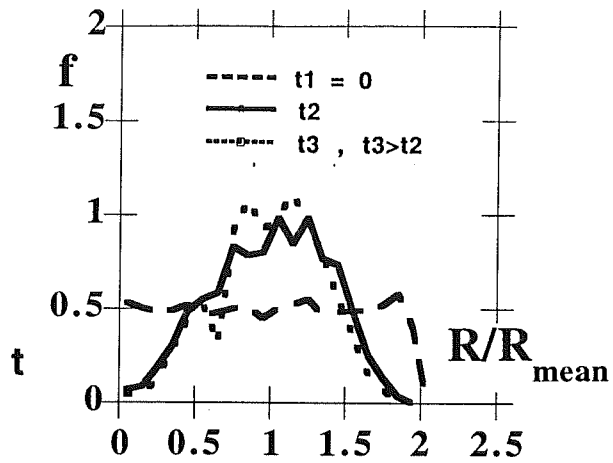


Figure 3 : Time evolution of the reduced particle size distribution ( $\phi = 0.25$  and constant diffusivity)

Figure 4 represents the kinetic constant of the cubic law  $K$  versus the volume fraction  $\phi$  for  $\phi$  values between 0.02 and 0.95. The shape of the curve  $K(\phi)$  can be explained in the framework of the De Hoff's theory (13, 17). Below the value of 0.02, the mean radius versus time does not obey a cubic law. Both the standard deviation and the skewness take stable values after relatively rapid changes in the early stages of coarsening. These stable values are not highly dependent upon the volume fraction ( $\sigma_{qs} = 0.34 \pm 0.02$  ;  $S_{qs} = -0.25 \pm 0.05$ ).

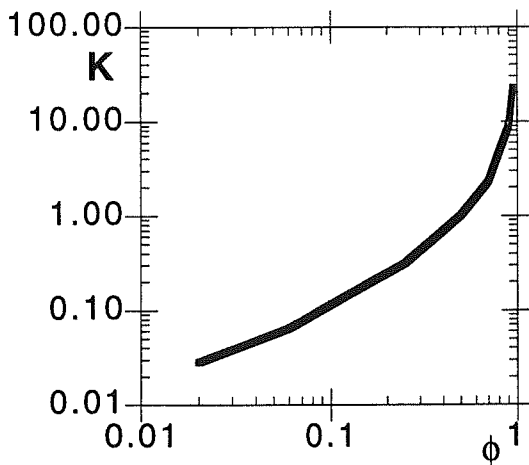


Figure 4 : Kinetic constant of the cubic law versus the volume fraction at constant diffusivity

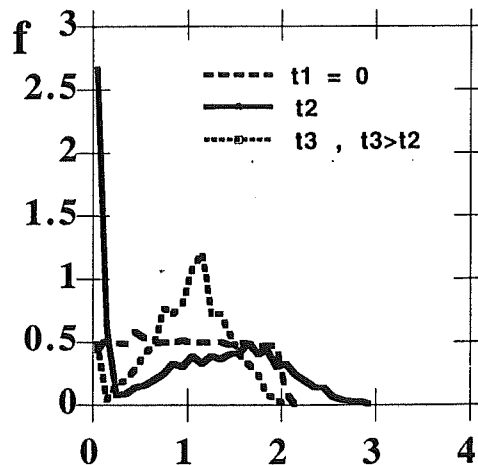


Figure 5 : Time evolution of the PSD ( $\phi = 0.25$  and concentration dependent diffusivity)

#### Diffusivity dependent on solute concentration.

When the solute diffusion is the rate-limiting step, a cubic law is observed too; the dimensionless kinetic constant is slightly smaller :  $2.65 \cdot 10^{-7}$  instead of  $3.16 \cdot 10^{-7}$  for a volume fraction equal to 0.25. In fact, the supersaturation is very close to one ; hence the diffusivity becomes closed to  $D_{eq}^\infty$ . On the other hand, the shape of the PSD is very different (Fig. 5). We observe the presence of the smallest grains,

particularly at the beginning of ripening. This is due to a slower disappearance of small grains because of the low value of the solute diffusivity in their neighbourhood. Nevertheless, the peak due to the smallest grains decreases in the long run.

### TRANSIENT BEHAVIOUR

Our model is particularly useful to the study of the first instants of the ripening. We already have studied the influence of the initial PSD, and the influence of the initial particles arrangement (17). For example, if all the particles, but one, have the same size  $R_0$ , we can observe the propagation of a mass wave ; in a recent paper (26) we have shown the occurrence of a coherent region behind the propagation front. This coherent region contains a constant particle number with the same radius equal to  $2R_0$ .

In the early stage of coarsening, one of the relevant parameters is a "smoothing function" of the particles set.

The simplest way to define the "smoothing function"  $q_f$  is:

$$q_f^2 = \frac{1}{N} \sum_{i=1}^N \left( \frac{2R_i - R_{i-1} - R_{i+1}}{R} \right)^2$$

Figure 6 shows the variation of  $q_f$  with time for the two kinds of diffusivity. In the two cases,  $q_f$  tends to an asymptotic value equal to 0.8, corresponding to the quasi stable state. When the diffusivity is depending on concentration, the transient period is longer and the smoothing function variations are large. We also observe the same behaviour for the variation of  $\bar{R}^3 - R_0^3$  with time (Fig. 7). As the small grains slowly disappear (because of the low diffusivity), the mean radius does not increase, thus the size difference between the smallest and the biggest grains remains large, and  $q_f$  increases.

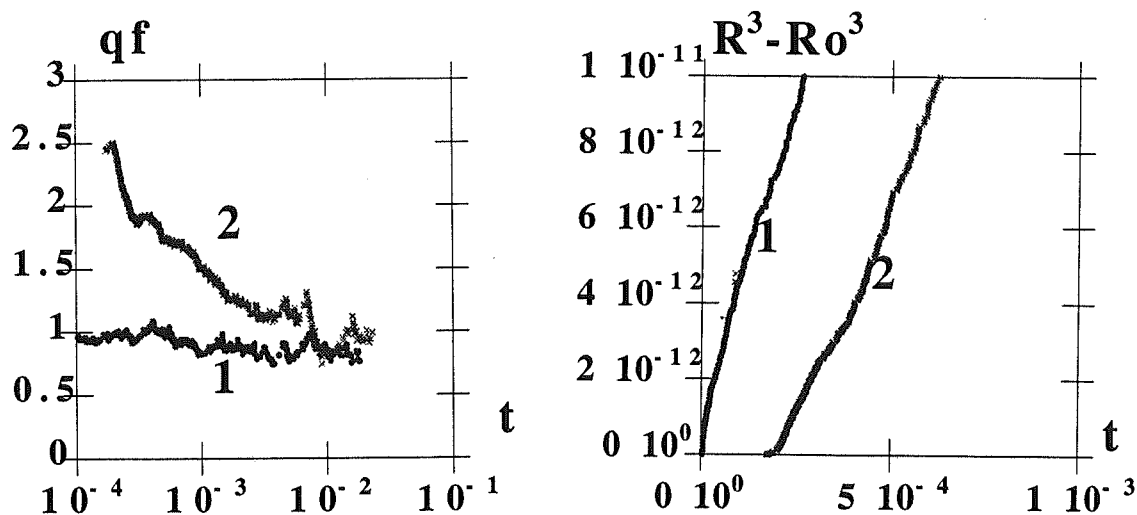


Figure 6 : Smoothing parameter vs time  $t$  ( $\phi = 0.25$  ; Figure 7 :  $\bar{R}^3 - R_0^3$  versus time  $t$  ( $\phi = 0.25$  ; dimensionless variables) ; 1 : Constant D ; 2 :  $D(\rho_A)$  dimensionless variables) ; 1 : Constant D ; 2 :  $D(\rho_A)$

### CONCLUSION

Within a unidimensional model of Ostwald ripening, the main results already known on this phenomenon have been retrieved: asymptotic mean radius variation with time, quasi-stable PSD, ... In

addition to this, new aspects, never studied before have been investigated : influence of high volume fraction of highly soluble solids, effect of the spatial grain arrangement (which has been characterized via a "smoothing function"), existence of a coherent mass-wave propagation along the grain population, first stage of the ripening phenomenon, influence of a non-constant mass diffusion coefficient ; the results from recent works of Myerson et al. have been applied. Compared to the behaviour observed for constant diffusivity, ripening is considerably slowed down in its early stage, however the asymptotic behaviour is little affected apart from the presence of a tail of fine particles. Due to its simplicity and to the relative rapidity of the calculations, the present model can be used for a large variety of situations of Ostwald ripening.

## REFERENCES

1. Todes, O.M., J. Phys. Chem. (Sov.), 20, 629 (1946).
2. Lifshitz, I.M. and V.V. Slyosov, J. Phys. Chem. Solids, 19, 35 (1961).
3. Wagner, C., Zeitschrift für Elektrochemie, 65, 581 (1961).
4. Asimow, R., Acta Metall., 11, 72 (1963).
5. Ardell, A.J. Acta Metall., 20, 61 (1972).
6. Brailsford, A.D. and P. Wynblatt, Acta Metall., 27, 489 (1979).
7. Tsumuraya, K and Y. Miyata, Acta Metall., 31, 437 (1983).
8. Marqusee, J.A., Chem. Phys., 81, 976 (1984).
9. Weins, J.J. and J.W. Cahn, Sintering and Related Phenomena, Plenum, New-York (1973), p. 151.
10. Voorhees, P.W. and M.E. Glicksman, Acta Metall., 32, 2001 (1984).
11. Voorhees, P.W. and M.E. Glicksman, Acta Metall., 32, 2013 (1984).
12. Voorhees, P.W. and M.E. Glicksman, Metall. Trans. A, 15A, 1081 (1984).
13. Dehoff, R.T., Acta Metall. Mater., 39, 2349 (1991).
14. Fang, Z., B.R. Patterson and M.E. Turner, Acta Metall. Mater., 40, 713 (1992).
15. Brown, L.C. Acta Metall. Mater., 37, 71 (1989).
16. Brown, L.C. Acta Metall. Mater., 40, 1293 (1992).
17. Gruy, F. and M. Cournil, Acta Metall. Mater., in press.
18. Chang, Y.C. and A.S. Myerson, AIChE Journal, 31, 890 (1985).
19. Newman, J. and T.W. Chapman, AIChE Journal, 19, 343 (1973).
20. Robinson, R.A. and R.H. Stokes, Electrolyte solutions, Ed. Butterworths (1968).
21. Pascal, P., Nouveau traité de chimie minérale, Masson, Paris (1966).
22. Vrentas, J.S., and C.M. Vrentas, Chem. Eng. Sci., 44, 3001 (1989).
23. Chatterjee, S.G. and C. Tien, Chem. Eng. Sci., 44, 2283 (1989).
24. Sudhakar, B., Chem. Eng. Sci., 47, 475 (1992).
25. Fang, Z. and B.R. Patterson, Acta Metall. Mater., 41, 2017 (1993).
26. Gruy, F. and M. Cournil, C.R. Acad. Sci. Paris, t 321, Serie IIb, p. 187 (1995).